Controlling the recovery time of the superconducting nanowire single-photon detector with a voltage-controlled cryogenic tunable resistor

Wang, H.; Orlov, N. D.; Noordzij, N.; Descamps, T.; Los, J. W.N.; Zwiller, V.

DOI
10.1063/5.0297362

Publication date
2025

Document Version
Final published version

Published in
Applied Physics Letters

Applied Physics Letters

RESEARCH ARTICLE | NOVEMBER 25 2025

Controlling the recovery time of the superconducting nanowire single-photon detector with a voltage-controlled cryogenic tunable resistor

H. Wang ; N. D. Orlov ; N. Noordzij; T. Descamps ; J. W. N. Los; V. Zwiller ; I. Esmaeil Zadeh

Appl. Phys. Lett. 127, 212601 (2025)
https://doi.org/10.1063/5.0297362

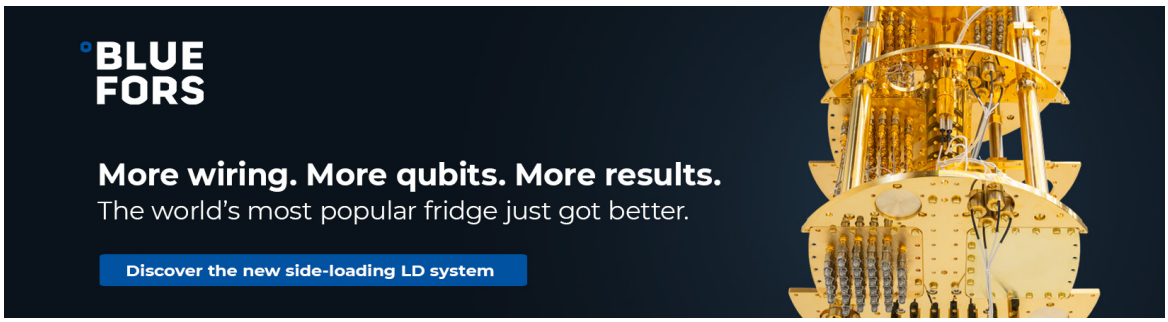

AIP Publishing

Applied Physics Letters ARTICLE pubs.aip.org/aip/apl

Controlling the recovery time of the superconducting nanowire single-photon detector with a voltage-controlled cryogenic tunable resistor

Cite as: Appl. Phys. Lett. **127**, 212601 (2025); doi: 10.1063/5.0297362
Submitted: 19 August 2025 · Accepted: 10 November 2025 ·
Published Online: 25 November 2025

H. Wang,[1,a] N. D. Orlov,[1] N. Noordzij,[2] T. Descamps,[3] J. W. N. Los,[2] V. Zwiller,[3] and I. Esmaeil Zadeh[1,b]

AFFILIATIONS

[1]Department of Imaging Physics, Delft University of Technology, 2628 CN Delft, The Netherlands
[2]Single Quantum B.V., 2628 CH Delft, The Netherlands
[3]Department of Applied Physics, Royal Institute of Technology (KTH), SE-106 01 Stockholm, Sweden

[a]**Author to whom correspondence should be addressed:** h.wang-19@tudelft.nl
[b]**Also at:** Single Quantum B.V., 2628 CH Delft, The Netherlands.

ABSTRACT

Superconducting nanowire single-photon detectors (SNSPDs), owing to their unique performance, are currently the standard detector in most demanding single-photon experiments. One important metric for any single-photon detector is the recovery time, which defines the minimum temporal separation between consecutive detection events. In SNSPDs, the recovery time is more subtle, as the detection efficiency does not abruptly drop to zero when the temporal separation between detection events gets smaller, instead, it increases gradually as the SNSPD current recovers. SNSPD's recovery time is dominated by its kinetic inductance, the readout impedance, and the degree of saturation of internal efficiency. Decreasing the kinetic inductance or increasing the readout impedance can accelerate the recovery process. Significant reduction of the SNSPD recovery time, by, for example, adding a series resistor in the readout circuitry, is possible but can lead to detector latching, which hinders further detector operation or enforces underbiasing and hence a reduction in detection efficiency. Previous research has demonstrated passive resistive networks for the reduction of recovery time that rely on trial and error to find the appropriate resistance values. Here, we show that, using a cryogenically compatible and tunable resistor technology, one can find the optimized impedance values, delivering fast SNSPD recovery time while maintaining maximum internal detection efficiency. Here, we show an increase of around twofold in both maximum achievable detection rates and the achievable detection efficiency at high photon fluxes, demonstrating detection rates close to 114 Mcps with no loss of internal detection efficiency.

Superconducting nanowire single-photon detectors (SNSPDs), composed of superconducting nanowires biased close to their critical currents, have become a cutting-edge technology in single-photon detection.[1–3] SNSPDs have gained numerous research interests, attributed to their remarkable single-photon sensitivity, broad spectral range,[4,5] high detection efficiency (>95 %[6–8]), and low time jitter (tens of picoseconds[9–11]). There is an increasing demand for SNSPDs in various applications such as biomedical imaging,[12] optical communication,[13] and quantum key distribution.[14–16]

When a photon is absorbed by the SNSPD, a resistive section is formed in the nanowire, which will initially expand due to Joule heating. Subsequently, in an appropriately functioning SNSPD, the bias current is diverted to the readout, and this resistive section disappears due to the reduction of Joule heating and continuous cooling of the sample. These dynamics in the current redistribution between the SNSPD and the readout electronics lead to an electrical pulse at the output. The resulting output pulse usually rises steeply (sub-nanosecond) and decays slowly (nanoseconds), which is correlated with the inductive time constant L_k/R (L_k is the kinetic inductance of the SNSPD, which dominates its total inductance over the geometric inductance, and R is the resistance in the circuit). Thus, the falling edge of the output influences the nanowire current recovery time,

which is linked to its internal detection efficiency as a result. As the efficiency does not drop and recover abruptly in SNSPDs, the recovery time τ_{rec} can be defined as the time interval required to register a second photon subsequent to an earlier detection event with 50 % of the normalized detection efficiency. This parameter is one of the essential performance metrics for applications that demand higher photon count rates, such as optical communication or high-throughput optical quantum computing.

SNSPDs have a shorter recovery time when their kinetic inductances are lower, straightforwardly achieved by shortening the meander. However, this also results in the reduction of the active detection area, which is disadvantageous for optical absorption and hence system detection efficiency. Other approaches to raise detection rates, such as utilizing quasi-constant-voltage (QCV) bias[17] and implementing a DC-coupled readout scheme,[18] were demonstrated, but these non-cryogenic solutions have limited performance enhancements as there is a considerable delay (nanoseconds) between the SNSPD and the control circuit. Another more effective way is to introduce a cryogenic serial resistor to SNSPD's readout circuit to reduce the recovery time by increasing R.[19,20] The value of the serial resistance needs to be carefully optimized to minimize recovery time while avoiding the formation of a stable hot spot in the superconducting nanowire, which is referred to as the latching phenomenon.[21] Based on the analysis of electrothermal effects in SNSPDs, the optimized value for this serial resistance can be influenced by various factors such as the heat transfer coefficient between the superconducting nanowire and the substrate, the geometry of the meandering nanowire, and the material properties of the superconducting layer (sheet resistance, critical current density, biasing current, etc.).[22] Therefore, the resistance value is often refined experimentally through a series of trials and errors, which is time-consuming and does not necessarily guarantee optimal performance.

In this work, we demonstrate a cryogenic tunable resistor to tune the serial resistance to the optimal value. The tunable resistor consists of a superconducting channel and a metal heater insulated by a SiO_2 layer. The resistance of the superconducting channel is controlled by the localized heat transfer from the heater and the self-Joule heating of the superconducting channel. This adjustable electrical component operating in cryogenic environments constitutes an efficient strategy to enhance the SNSPD performance at high photon flux rates. We show that this on-chip device is fully compatible with SNSPDs, enabling real-time optimization of the electrical recovery time while maintaining high internal detection efficiency.

Figure 1 represents a one-dimensional electrothermal simulation as described in Yang *et al.*,[21] which illustrates the basic principle of decreasing the recovery time by connecting a small resistor in series with an SNSPD (more information about the simulation can be found in the supplementary material). The results were simulated at 2.5 K, which is the base temperature of our cryostat. An equivalent electrical diagram of an SNSPD in series with a resistor R_s is depicted in Fig. 1(a). The SNSPD is biased with a current source I_{bias} and is in parallel with the readout electronics, which is a capacitor C_b and a load resistor $Z_0 = 50\,\Omega$, representing the input impedance of an RF amplifier.

Once a single photon triggers a resistive section across the nanowire, this section quickly expands due to Joule heating, and the effective bias current through the detector I_d is redirected to the load resistor, resulting in the rising edge at the output. The characteristic time of the rising edge is $\tau_1(t) \approx L_k/(Z_0 + R_s + R_L(t))$, where

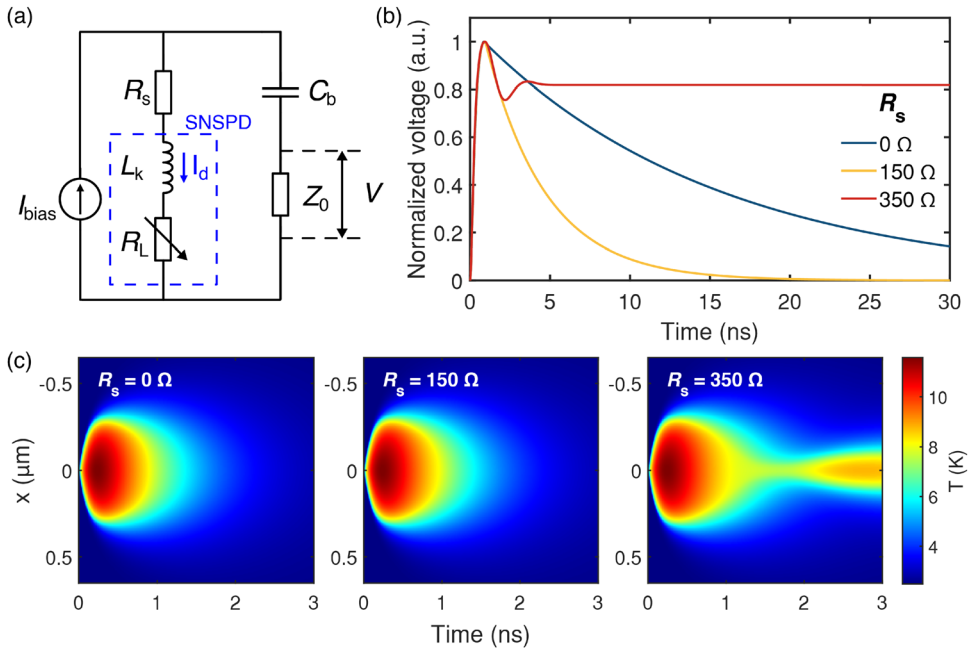

FIG. 1. (a) Schematic representation of electrical equivalent model of an SNSPD with a resistor R_s in series. (b) Simulated output voltage profile with $R_s = 0$, 150, and 350 Ω, respectively. (c) The evolution of the temperature profile of the superconducting nanowire with $R_s = 0$, 150, and 350 Ω, respectively. x is the spatial coordinate along the nanowire with the hot spot at the origin. Details of the simulation parameters can be found in the supplementary material.

$L_k = 750$ nH and $R_L(t)$ represent the kinetic inductance of the detector and the real-time total hot-spot resistance in our simulation, respectively. After the resistive spot disappears via the heat dissipation to the substrate, the current flows back to the SNSPD with the time constant $\tau_2 \approx L_k/(Z_0 + R_s)$, corresponding to the falling edge of the output signal. Since $R_L(t)$ (typically a few k Ω) significantly exceeds Z_0 and R_s, the pulse width τ_{out} defined at $1/e$ of the pulse height is dominated by τ_2.

The simulated output signals with three different R_s values are shown in Fig. 1(b). The pulse decay time (estimated via exponential fitting) reduces from 14.99 to 3.75 ns by increasing R_s from 0 to 150 Ω without changing the nanowire structure, which is consistent with the analytical expression of τ_2. However, for a larger value of $R_s = 350$ Ω, the detector latches to a non-superconducting state, as represented by the temperature profile in Fig. 1(c) (more information can be found in the supplementary material). In the latter case, the current returns to the SNSPD so rapidly that the resistive spot is sustained by reaching an equilibrium between heat generation via Joule heating in the nanowire and heat dissipation to the substrate.

The threshold of the serial resistance to avoid latching depends on both the electrical properties of the device, such as the kinetic inductance of the SNSPD, and the thermal properties of the materials, such as the heat transfer coefficient between the nanowire and the substrate. Unfortunately, measuring these properties accurately on different platforms is not straightforward and, therefore, it is non-trivial to predict the maximum R_s, which optimizes the current recovery while avoiding the latching or loss of internal efficiency. Using fixed resistors, the experimental testing and validation process can take a considerable amount of effort and time. Hence, here, we propose and demonstrate a cryogenic tunable resistor, as depicted in Fig. 2, which makes it convenient to optimize the SNSPD performance with a serial tunable resistor.

An illustration of an SNSPD in series with a tunable resistor, as well as the schematic of the associated readout electronics, is shown in Fig. 2(a). An optical micrograph of a representative tunable resistor is shown in Fig. 2(b), which consists of a metal strip (an 80-nm-thick Ti layer with a 5-nm-thick Au layer) fabricated over a superconducting channel (NbTiN, with a thickness of 8–10 nm) insulated by a thin SiO_2 layer (40–50 nm in thickness). The metal strip acts as a micro-heater once connected to an electric power supply, producing Joule heat and raising the local temperature. When the local temperature exceeds the critical temperature, a resistive strip is formed in the channel, which introduces a tunable resistance in the circuit. The channel is narrowed down as it approaches the center of the metal heater to constrict the expansion of the resistive area and prevent the channel from latching.

The resistance of the channel is determined by both the bias current through the superconducting channel, I_{bias}, and the heater current, I_h. In Fig. 2(c), we characterize the dependence of channel resistance R on the currents I_{bias} and I_h in the device (DC analysis). The minimum width of the NbTiN channel is 1 μm, which is larger than the meander width of the SNSPD (typically < 100 nm) to ensure that stray photons cannot trigger a hot spot in the channel, and the metal heater has a width of 0.3 μm. As the bias current through the superconducting channel increases, the resistance grows faster with the heater current. This behavior is due to the generation of Joule heat in the NbTiN channel $I_{bias}^2 R$, which becomes significant at higher bias currents. To ensure reliable tunability in the desired resistance range

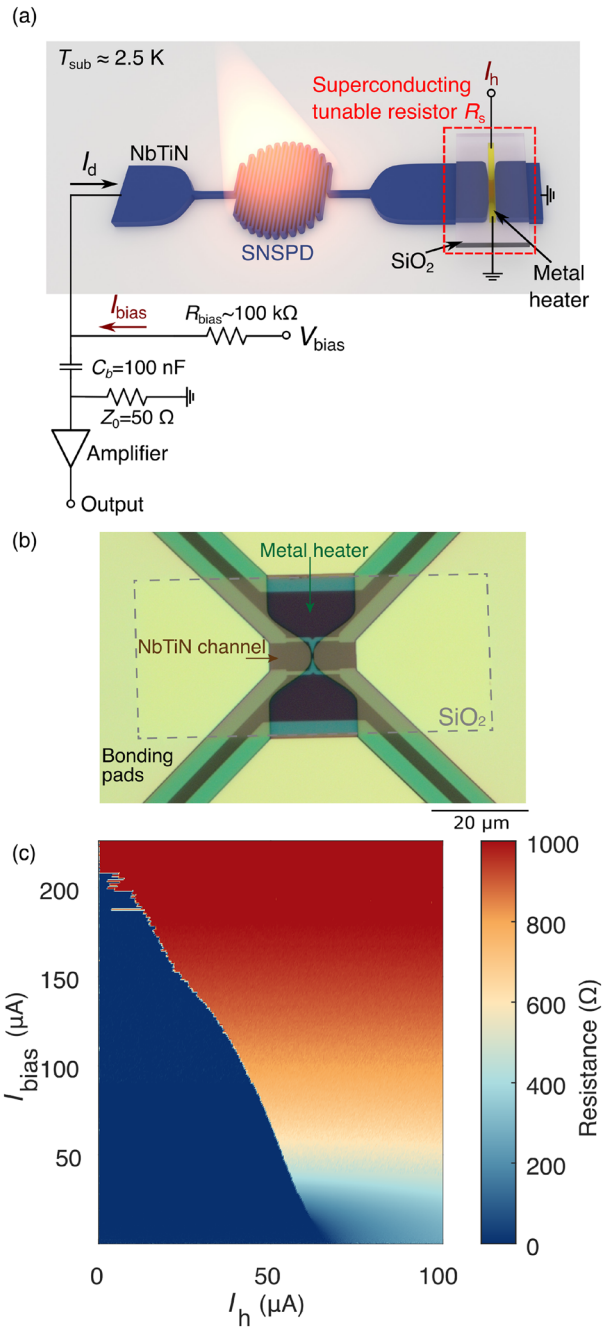

FIG. 2. (a) Illustration of a cryogenic tunable resistor R_s in series with an SNSPD and its electronic readout circuit. (b) Representative optical microscopy image of a cryogenic tunable resistor. (c) Characterization of the channel resistance in a cryogenic tunable resistor as a function of the channel bias current and the heater current. The channel has a width of 1 μm and the heater has a width of 300 nm.

(0–300 Ω), the tunable resistor is designed to operate at bias currents much lower than the switching current of the channel, typically around 5 % of the switching current depending on the heater and the channel geometry as well as the resistivity of the superconducting

material. More information about the stability of the channel resistance and the influence of the device geometry can be found in the supplementary material.

As depicted in Fig. 2(a), an SNSPD is connected in series with a cryogenic tunable resistor and biased and read out using a conventional bias tee and RF amplifiers. We characterize the sample in a flood illumination configuration with light injected from a fiber several centimeters above the sample. The output pulse is amplified and recorded using an oscilloscope. Both the theoretical analysis and the simulation results indicate that a higher I_h results in a shorter output pulse width τ_{out}, allowing two consecutive photons to, in principle, be detected with a shorter time delay. However, another crucial characteristic to consider is the detection efficiency of the second event, which itself depends on not only the current recovery speed but also on the degree of saturation of internal detection efficiency (IDE) (i.e., the relative length of the plateau in the detection efficiency curve to the switching current). Since the detection efficiency of SNSPD increases with the effective bias current, the probability of detecting a second photon grows as the current through the SNSPD recovers. Thus, we experimentally measured the recovery of the detection efficiency as a function of the time delay after the first detection event using continuous light sources at different heater currents (i.e., different serial resistances). The time when the normalized detection efficiency recovers to 50 % is estimated as the recovery time τ_{rec}.

Figure 3 shows the experimental results of an SNSPD composed of a 70-nm-wide nanowire in series with a cryogenic tunable resistor with a 1-μm-wide channel and a 0.3-μm-wide heater. The SNSPD was biased at around 90 % of the switching current and measured at a

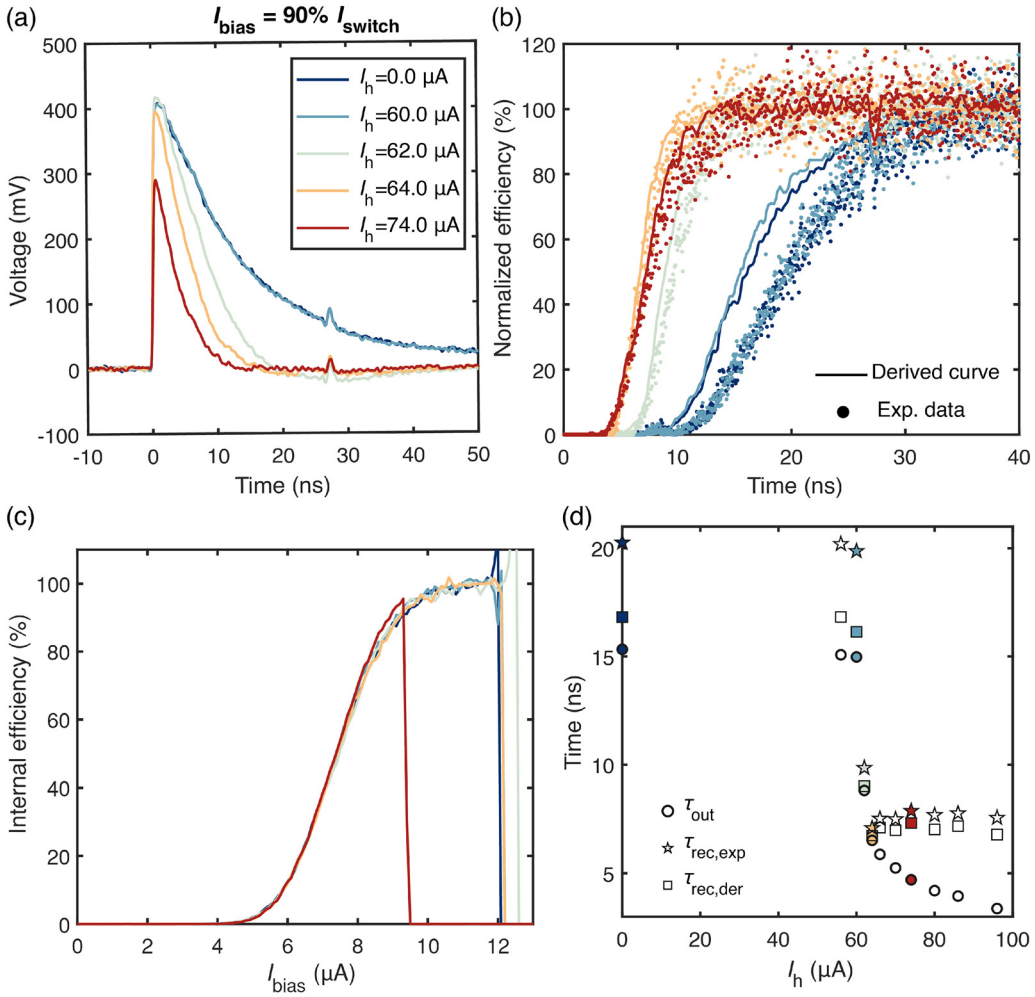

FIG. 3. (a) Amplified output waveforms of the SNSPD (curves are averaged over 100 sweeps). Comparison of the averaged and the single-sweep waveform can be found in the supplementary material. (b) Histogram of the normalized detection efficiency as a function of the time delay after one detection event with various I_h for the wavelength of 1548 nm. The filled dots represent the experimental data, and the solid ones are the predicted efficiency recovery curves derived from internal detection efficiency curves and output pulses. (c) Normalized internal detection efficiency curves with various heater currents I_h, obtained for the wavelength of 1548 nm. (d) Comparison of the output pulse recovery times width τ_{out} (measured at $1/e$ of the pulse amplitude), the experimental recovery time $\tau_{rec,exp}$, and the derived recovery time $\tau_{rec,der}$. $\tau_{rec,exp}$ or $\tau_{rec,der}$ is obtained by fitting the experimental data or the derived curve with the sigmoid function $y = A(1 + \mathrm{erf}(S(x - x_0)))$, where x_0 represents the fitted recovery time.

wavelength of 1548 nm. Figure 3(a) shows the recorded output pulses for various heater currents I_h. The experimental pulse widths match the trend in the simulation results. As the serial resistance increases by setting a higher heater current, the output pulse width declines from 15.3 ns at $I_h = 0\,\mu$A to 4.7 ns at $I_h = 74\,\mu$A. The falling time constant, obtained by exponential fitting of the falling edge, reduces from 13.85 ns at $I_h = 0\,\mu$A to 4.04 ns at $I_h = 74\,\mu$A, leading to a theoretical estimation of $R_s = 121.4\Omega$ at $I_h = 74\,\mu$A.

However, the efficiency recovery time does not monotonically decrease as the serial resistance increases. We experimentally measured the efficiency recovery curve (filled dots) as shown in Fig. 3(b) (see the measuring approach in the supplementary material). The experimental recovery time $\tau_{rec,exp}$ is obtained by fitting the experimental data to the sigmoid function $y = A(1 + \mathrm{erf}(S(x - x_0)))$, where x_0 indicates the fitted recovery time. $\tau_{rec,exp}$ is suppressed from 20.3 ns at $I_h = 0\,\mu$A to 7.1 ns at $I_h = 64\,\mu$A, which is consistent with the declining trend of the output pulse width. However, the recovery time increases to 7.9 ns at $I_h = 74\,\mu$A although τ_{out} becomes shorter. This results from the degradation of the internal detection efficiency of the detector. Figure 3(c) shows the internal detection efficiency (IDE) curves as a function of the bias current, which are normalized to the saturated efficiency estimated by fitting to the sigmoid function.[23] Since $I_h = 74\,\mu$A leads to an unsaturated IDE curve, a higher ratio of the effective bias current to the switching current I_d/I_{switch}, corresponding to a longer delay between two events, is required to achieve the same detection probability. This effect counteracts the influence of the shorter output pulse width, leading to a worse efficiency recovery time at $I_h = 74\,\mu$A.

Since the power consumption of a cryogenic tunable resistor ($< 3\,\mu$W) is much lower than the cooling power of the cryostat (~ 130 mW), the influence of local heating on the SNSPD performance can be dismissed (see the supplementary material). The change in the IDE curves is attributed to the decrease in the switching current $I_{switch} = \min\{I_c, I_{latch}\}$, where I_c is the critical current determined by the geometry of the nanowire and the critical current density of the superconducting film, and I_{latch} is the latching current at which the resistive spot in the superconducting nanowire is retained. As the output pulse width τ_{out} decreases, I_{latch} declines and eventually drops below I_c.[18,24] This results in the reduction of I_{switch}, restricting the bias current from approaching the critical current. Consequently, the saturation plateau of the internal detection efficiency diminishes as R_s exceeds an optimal value. The switching current increases slightly at $I_h = 62\,\mu$A, which is consistently observed in multiple datasets. This phenomenon may result from voltage attenuation across the serial tunable resistor, which suppresses reflections in the SNSPD circuit.

Furthermore, we investigate the recovery of the instantaneous detection efficiency derived from the output pulses and the IDE curve in Figs. 3(a) and 3(c).[25] The instantaneous effective bias current can be estimated using $I_d(t) = I_{bias} - V_{out}(t)/G/Z_0$, where $V_{out}(t)$ is the output pulse and $G = 10^{2.9}$ is the measured gain of our amplifier. Combined with the IDE curve $\eta = f(I_d)$, the instantaneous detection efficiency can be derived as $\eta(t) = f(I_d(t))$, which is shown as solid lines in Fig. 3(b). Similar to the acquisition of the experimental recovery time, the derived recovery time $\tau_{rec,der}$ can be estimated by fitting the derived curve $\eta(t) = f(I_d(t))$ with the sigmoid function. Figure 3(d) shows the comparison between the pulse width τ_{out}, the experimental recovery time $\tau_{rec,exp}$, and the derived recovery time $\tau_{rec,der}$ at various heater currents. The result indicates that there is an optimal heater current I_h at 64 μA, that is, an optimal serial resistance R_s, where the efficiency recovery time can be minimized by reducing the pulse width. Discrepancies between $\tau_{rec,der}$ and $\tau_{rec,exp}$ are probably caused by inaccurate estimations of effective bias currents or the triggering threshold for the second detection event (hysteresis settings of the counter's Schmitt trigger), which omits some events because of their lower amplitude or background noise (see the supplementary material). Nevertheless, $\tau_{rec,der}$ and $\tau_{rec,exp}$ show similar tendencies with respect to I_h, and exhibit good agreement under conditions of rapid efficiency recovery. Therefore, analyzing $\tau_{rec,der}$ can be considered a time-efficient approach to optimize the serial tunable resistor.

In order to further investigate the effect of recovery time reduction, we characterize the SNSPD detection efficiency at high count rates illuminated with a pulsed light source at 1548 nm at different heater currents. The detection efficiency, for each input photon flux, is calculated using the count rates at 95 % of the switching current. Examples of the measurement curves (count rate vs bias current at different input photon fluxes) are presented in the supplementary material. The analyzed results are shown in Fig. 4 for the laser

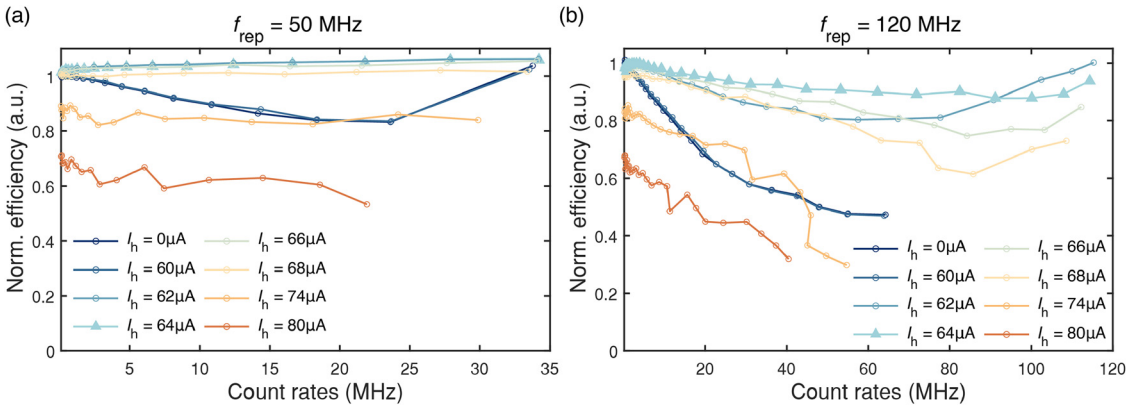

FIG. 4. Normalized detection efficiency as a function of detection count rates at various heater currents I_h with a repetition rate of (a) $f_{rep} = 50$ and (b) $f_{rep} = 120$ MHz. For each laser repetition rate, the best detector performance can be achieved by tuning the heater current. Measurements at $I_h = 64\,\mu$A, which consistently delivers near-optimal or optimal performances across a broad range of count rates, are highlighted with triangles for a better display.

repetition rates of 50 and 120 MHz. Note that the data in Fig. 4 are normalized with respect to the efficiency at the lowest input photon flux (lowest count rate) when $I_h = 0\,\mu$A (more measurements can be found in the supplementary material).

According to the measurement in Fig. 3(d), the recovery time of the SNSPD is longer or comparable to $1/f_{rep}$ at lower heater currents than 60 μA. Thus, the detection efficiencies for these lower heater currents decrease as the count rate increases (due to the insufficient current recovery through the SNSPD). When the count rates increase beyond half of f_{rep}, the efficiency exhibits an upward tendency, which is attributed to the increase in SNSPD current via parasitic discharging currents of the readout capacitor.[26] The parasitic currents flowing back through the SNSPD enhance the effective bias currents and thus the detection efficiency.

As the heater current increases, the best efficiency performance over a broad range of count rates is achieved at $I_h = 64\,\mu$A, which is in accordance with the recovery time measurement. When the heater current exceeds 64 μA, the efficiency declines steadily due to the unsaturated IDE (see the supplementary material). At $f_{rep} = 50$ MHz and $I_h = 64\,\mu$A, the detection efficiency is maintained around the highest level at various count rates, since the minimal time delay between two pulses, which is 20 ns, is significantly longer than the recovery time $\tau_{rec,\,exp} = 7.1$ ns, resulting in complete recovery of the effective bias current for all detection events. As the minimum separation between incident photons for the case of $f_{rep} = 120$ MHz approaches the recovery time (at $I_h = 64\,\mu$A), and the efficiency recovery is not fully completed, a slight decline in efficiency can be observed at higher count rates. Nevertheless, the normalized detection efficiency remains at around 90% until a count rate of 114.2 MHz at $I_h = 64\,\mu$A for $f_{rep} = 120$ MHz, while the normalized detection efficiency is decreased to 50% with a count rate of 48.0 MHz at $I_h = 0\,\mu$A. Thus, there is a twofold increase in the maximum detection count rate.

In conclusion, we demonstrated a cryogenic tunable resistor controlled by the localized micro-heater. The device is intrinsically cryogenic-compatible and suitable for integration with other superconducting devices. We showed that, by controlling the tunable resistor in series with an SNSPD, the efficiency recovery time of the detector can be tuned to enhance detection efficiency at high count rates. Compared with trial-and-error-based fixed resistive networks, the cryogenic tunable resistor significantly speeds up the optimization process and can be adapted to a variety of SNSPD geometries or materials. Our solution provides a convenient method to tune SNSPD performance at higher photon fluxes. In addition, the tunable resistor presented here has the potential to be integrated with other cryogenic technologies.

See the supplementary material for details on sample fabrication, DC characteristics of the cryogenic tunable resistor, electrothermal simulation of an SNSPD with a serial resistor, the approach to measure efficiency recovery curves, more results of high-count-rate measurements, additional information about SNSPD output pulses, and measurements of the FWHM jitter.

I.E.Z. and H.W. acknowledge the funding from the FREE project (P19-13) of the TTW-Perspectief research program partially financed by the Dutch Research Council (NWO); I.E.Z. acknowledges funding from the European Union's Horizon Europe research and innovation programme under Grant Agreement No. 101098717 (RESPITE project) and No. 101099291 (fastMOT project).

AUTHOR DECLARATIONS

Conflict of Interest

N. Noordzij (full time), J. W. Niels Los (full time) and I. Esmaeil Zadeh (part-time) are employed by Single Quantum B. V. and may profit financially. The authors have no conflicts to disclose.

Author Contributions

H. Wang: Conceptualization (equal); Data curation (equal); Formal analysis (equal); Investigation (lead); Methodology (equal); Resources (equal); Software (equal); Supervision (equal); Validation (equal); Visualization (equal); Writing – original draft (equal); Writing – review & editing (equal). **N. D. Orlov:** Data curation (equal); Formal analysis (equal); Investigation (equal); Writing – original draft (equal); Writing – review & editing (equal). **N. Noordzij:** Investigation (equal); Methodology (equal); Resources (equal); Writing – original draft (equal); Writing – review & editing (equal). **T. Descamps:** Investigation (equal); Resources (equal); Writing – original draft (equal); Writing – review & editing (equal). **J. W. N. Los:** Conceptualization (equal); Supervision (equal); Validation (equal); Writing – original draft (equal); Writing – review & editing (equal). **V. Zwiller:** Supervision (equal); Writing – original draft (equal); Writing – review & editing (equal). **I. Esmaeil Zadeh:** Conceptualization (equal); Funding acquisition (equal); Investigation (equal); Methodology (equal); Project administration (equal); Supervision (equal); Validation (equal); Visualization (equal); Writing – original draft (equal); Writing – review & editing (equal).

DATA AVAILABILITY

The data that support the findings of this study are available from the corresponding author upon reasonable request.

REFERENCES

[1]G. N. Gol'tsman, O. Okunev, G. Chulkova, A. Lipatov, A. Semenov, K. Smirnov, B. Voronov, A. Dzardanov, C. Williams, and R. Sobolewski, "Picosecond superconducting single-photon optical detector," Appl. Phys. Lett. **79**, 705–707 (2001). https://pubs.aip.org/aip/apl/article-pdf/79/6/705/8782545/705_1_online.pdf.

[2]J. A. Lau, V. B. Verma, D. Schwarzer, and A. M. Wodtke, "Superconducting single-photon detectors in the mid-infrared for physical chemistry and spectroscopy," Chem. Soc. Rev. **52**, 921–941 (2023).

[3]F. P. Venza and M. Colangelo, "Research trends in single-photon detectors based on superconducting wires," APL Photonics **10**, 040901 (2025).

[4]Y. Pan, H. Zhou, X. Zhang, H. Yu, L. Zhang, M. Si, H. Li, L. You, and Z. Wang, "Mid-infrared Nb_4N_3-based superconducting nanowire single photon detectors for wavelengths up to 10 μm," Opt. Express **30**, 40044–40052 (2022).

[5]M. Colangelo, A. B. Walter, B. A. Korzh, E. Schmidt, B. Bumble, A. E. Lita, A. D. Beyer, J. P. Allmaras, R. M. Briggs, A. G. Kozorezov, E. E. Wollman, M. D. Shaw, and K. K. Berggren, "Large-area superconducting nanowire single-photon detectors for operation at wavelengths up to 7.4 μm," Nano Lett. **22**, 5667–5673 (2022). pMID: 35848767.

[6]J. Chang, J. W. N. Los, J. O. Tenorio-Pearl, N. Noordzij, R. Gourgues, A. Guardiani, J. R. Zichi, S. F. Pereira, H. P. Urbach, V. Zwiller, S. N. Dorenbos, and I. Esmaeil Zadeh, "Detecting telecom single photons with $(99.5^{+0.5}_{-2.07})$ % system detection efficiency and high time resolution," APL Photonics **6**, 036114 (2021).

[7]D. V. Reddy, R. R. Nerem, S. W. Nam, R. P. Mirin, and V. B. Verma, "Superconducting nanowire single-photon detectors with 98% system detection efficiency at 1550 nm," Optica **7**, 1649–1653 (2020).
[8]P. Hu, H. Li, L. You, H. Wang, Y. Xiao, J. Huang, X. Yang, W. Zhang, Z. Wang, and X. Xie, "Detecting single infrared photons toward optimal system detection efficiency," Opt. Express **28**, 36884–36891 (2020).
[9]B. Korzh, Q.-Y. Zhao, J. P. Allmaras, S. Frasca, T. M. Autry, E. A. Bersin, A. D. Beyer, R. M. Briggs, B. Bumble, M. Colangelo, G. M. Crouch, A. E. Dane, T. Gerrits, A. E. Lita, F. Marsili, G. Moody, C. Peña, E. Ramirez, J. D. Rezac, N. Sinclair, M. J. Stevens, A. E. Velasco, V. B. Verma, E. E. Wollman, S. Xie, D. Zhu, P. D. Hale, M. Spiropulu, K. L. Silverman, R. P. Mirin, S. W. Nam, A. G. Kozorezov, M. D. Shaw, and K. K. Berggren, "Demonstration of sub-3 ps temporal resolution with a superconducting nanowire single-photon detector," Nat. Photonics **14**, 250–255 (2020).
[10]G. G. Taylor, E. N. MacKenzie, B. Korzh, D. V. Morozov, B. Bumble, A. D. Beyer, J. P. Allmaras, M. D. Shaw, and R. H. Hadfield, "Mid-infrared timing jitter of superconducting nanowire single-photon detectors," Appl. Phys. Lett. **121**, 214001 (2022).
[11]J. Chang, I. E. Zadeh, J. W. N. Los, J. Zichi, A. Fognini, M. Gevers, S. Dorenbos, S. F. Pereira, P. Urbach, and V. Zwiller, "Multimode-fiber-coupled superconducting nanowire single-photon detectors with high detection efficiency and time resolution," Appl. Opt. **58**, 9803–9807 (2019).
[12]F. Xia, M. Gevers, A. Fognini, A. T. Mok, B. Li, N. Akbari, I. E. Zadeh, J. Qin-Dregely, and C. Xu, "Short-wave infrared confocal fluorescence imaging of deep mouse brain with a superconducting nanowire single-photon detector," ACS Photonics **8**, 2800–2810 (2021).
[13]F. Bellei, A. P. Cartwright, A. N. McCaughan, A. E. Dane, F. Najafi, Q. Zhao, and K. K. Berggren, "Free-space-coupled superconducting nanowire single-photon detectors for infrared optical communications," Opt. Express **24**, 3248–3257 (2016).
[14]K. Takemoto, Y. Nambu, T. Miyazawa, Y. Sakuma, T. Yamamoto, S. Yorozu, and Y. Arakawa, "Quantum key distribution over 120 km using ultrahigh purity single-photon source and superconducting single-photon detectors," Sci. Rep. **5**, 14383 (2015).
[15]F. Grünenfelder, A. Boaron, G. V. Resta, M. Perrenoud, D. Rusca, C. Barreiro, R. Houlmann, R. Sax, L. Stasi, S. El-Khoury, E. Hänggi, N. Bosshard, F. Bussières, and H. Zbinden, "Fast single-photon detectors and real-time key distillation enable high secret-key-rate quantum key distribution systems," Nat. Photonics **17**, 422–426 (2023).
[16]F. Beutel, H. Gehring, M. A. Wolff, C. Schuck, and W. Pernice, "Detector-integrated on-chip QKD receiver for GHz clock rates," npj Quantum Inf. **7**, 40 (2021).
[17]D.-K. Liu, S.-J. Chen, L.-X. You, Y.-L. Wang, S. Miki, Z. Wang, X.-M. Xie, and M.-H. Jiang, "Nonlatching superconducting nanowire single-photon detection with quasi-constant-voltage bias," Appl. Phys. Express **5**, 125202 (2012).
[18]A. J. Kerman, D. Rosenberg, R. J. Molnar, and E. A. Dauler, "Readout of superconducting nanowire single-photon detectors at high count rates," J. Appl. Phys. **113**, 144511 (2013).
[19]Q. Zhao, T. Jia, M. Gu, C. Wan, L. Zhang, W. Xu, L. Kang, J. Chen, and P. Wu, "Counting rate enhancements in superconducting nanowire single-photon detectors with improved readout circuits," Opt. Lett. **39**, 1869–1872 (2014).
[20]C. L. Lv, H. Zhou, H. Li, L. X. You, X. Y. Liu, Y. Wang, W. J. Zhang, S. J. Chen, Z. Wang, and X. M. Xie, "Large active area superconducting single-nanowire photon detector with a 100 μm diameter," Supercond. Sci. Technol. **30**, 115018 (2017).
[21]J. K. W. Yang, A. J. Kerman, E. A. Dauler, V. Anant, K. M. Rosfjord, and K. K. Berggren, "Modeling the electrical and thermal response of superconducting nanowire single-photon detectors," IEEE Trans. Appl. Supercond. **17**, 581–585 (2007).
[22]A. J. Kerman, J. K. W. Yang, R. J. Molnar, E. A. Dauler, and K. K. Berggren, "Electrothermal feedback in superconducting nanowire single-photon detectors," Phys. Rev. B **79**, 100509 (2009).
[23]C. Autebert, G. Gras, E. Amri, M. Perrenoud, M. Caloz, H. Zbinden, and F. Bussières, "Direct measurement of the recovery time of superconducting nanowire single-photon detectors," J. Appl. Phys. **128**, 074504 (2020).
[24]I. Craiciu, B. Korzh, A. D. Beyer, A. Mueller, J. P. Allmaras, L. Narváez, M. Spiropulu, B. Bumble, T. Lehner, E. E. Wollman, and M. D. Shaw, "High-speed detection of 1550 nm single photons with superconducting nanowire detectors," Optica **10**, 183–190 (2023).
[25]L. Oshiro, H. Jones, T. Rambo, J. Cassada, S. Boyd, and A. Miller, "Accurately modeling the recovery time of superconducting nanowire single-photon detectors as a function of bias current," Proc. SPIE **13391**, 133910Z (2025).
[26]S. Ferrari, V. Kovalyuk, A. Vetter, C. Lee, C. Rockstuhl, A. Semenov, G. Gol'tsman, and W. Pernice, "Analysis of the detection response of waveguide-integrated superconducting nanowire single-photon detectors at high count rate," Appl. Phys. Lett. **115**, 101104 (2019).